J Wood Sci (2009) 55:323–328
DOI 10.1007/s10086-009-1041-5

ORIGINAL ARTICLE

Hiroki Sakagami · Junji Matsumura · Kazuyuki Oda

In situ visualization of hardwood microcracks occurring during drying

Received: January 19, 2009 / Accepted: May 27, 2009 / Published online: July 17, 2009

Abstract Microcracks produced in an Acacia hybrid (*Acacia mangium* × *Acacia auriculiformis*) and *Melia azedarach* during drying were visualized in situ using confocal laser scanning microscopy (CLSM); the morphological differences were compared. In the Acacia hybrid, numerous microcracks were found between the wood fiber and ray parenchyma, which propagated toward both the pith and bark. The microcracks closed with further drying, but persisted until the last stage of drying. In *Melia azedarach*, however, few microcracks formed between the wood fiber and ray parenchyma in the latewood region; they also propagated toward both the pith and bark. Because the microcracks subsequently closed, some could not be detected by CLSM. These morphological characteristics resulted from differences in the wood structure and we conclude that the interface zone between the wood fiber and ray parenchyma is one type of weak point on the transverse surface that is susceptible to checking.

Key words Microcrack · Hardwood · Acacia hybrid (*A. mangium* × *A. auriculiformis*) · *Melia azedarach* · Confocal laser scanning microscopy

H. Sakagami (✉)
Department of Forest and Forest Products Sciences, Graduate School of Bioresource and Bioenvironmental Sciences, Kyushu University, 6-10-1 Hakozaki, Higashi-ku, Fukuoka 812-8581, Japan
Tel. +81-92-642-2982; Fax +81-92-642-2982
e-mail: h-sakagami@agr.kyushu-u.ac.jp

J. Matsumura · K. Oda
Department of Forest and Forest Products Sciences, Faculty of Agriculture, Kyushu University, Fukuoka 812-8581, Japan

Part of this report was presented at the 57th Annual Meeting of the Japan Wood Research Society, Hiroshima, Japan, August 2007, at the 25th Annual Meeting of the Wood Technological Association of Japan, Asahikawa, Japan, September 2007, at the 15th Annual Meeting of Japan Wood Research Society Kyusyu Branch, Oita, Japan, July 2008, and at the 9th Pacific Rim Bio-Based Composites Symposium, Rotorua, New Zealand, November 2008

Introduction

Checking due to drying is the most serious flaw in wood that compromises the quality of various wood products. The value of these damaged products decreases not only due to deterioration of the physical properties but also due to the obvious disfigurement. Many scientists have studied checking due to drying and have suggested ways to prevent it. Numerous drying methods have been suggested, each employing different temperatures, relative humidities, and drying schedules.[1] These investigations were aimed at finding methods of diminishing the checks forming during the final stage of drying. It has been suggested that the drying of wood results in damage at the ultrastructural level,[2,3] and microcracks invisible to the naked eye might form during the initial stage of drying.[4] In fact, the formation of microcracks due to drying of wood has been confirmed at the microscopic level.[5,6] In general, the checks along the orientation of the microfibrils in the S_2 layer are measured to determine the microfibril angle.[7] Wahl et al.[5] and Perré[6] observed that some of microcracks on the surface tended to close at the final stage of drying. Therefore, it is assumed that microcracks had already been generated on the surface even though they are not detected in the final stage of drying. Kifetew et al.[2] also observed the fractures by subjecting the wood to a tensile load and compared this effect in green wood and oven-dry/resoaked wood using scanning electron microscopy on the basis of the hypothesis that cell wall damage occurred due to drying. They pointed out that the strength of dried/resoaked woods was generally lower than that of the green woods.

It is important to understand the mechanism of microcrack formation in order to find measures to reduce its occurrence. In particular, in situ observation is essential because microcrack transformation is a continuous process. Furthermore, it is difficult to detect where and under what conditions they occur. Additionally, the extent of the damage cannot be determined unless the maximum size and number of microcracks is known. In a previous study, microcrack propagation was successfully visualized in situ

in *Cryptomeria japonica*, which is the most widely used softwood in Japan, from water-saturated to air-dry conditions using confocal laser scanning microscopy (CLSM).[8] This system enables in situ observation during drying under controlled temperature and relative humidity conditions. The findings of this study indicated that microcracks are generated between the ray parenchyma and tracheid in the latewood region and that they propagate in both the bark and pith directions along the ray parenchyma. Subsequently, the microcracks closed regardless of the decrease in the moisture content, and most could not be detected using CLSM at the last stage of drying. Similar morphologic changes were observed by Perré[6] in microcracks forming in Douglas fir; microcrack propagation was also observed in hardwoods. However, the magnification levels used were too low to accurately detect the microcracks at the cellular level.

The interest in fast-growing trees has recently increased and their wood qualities have been investigated by many scientists. While numerous investigations have been conducted on softwood species, investigations on hardwood species such as *Populus*, *Eucalyptus*, and *Acacia* have been few. However, hardwood species are being increasingly investigated given the recent rise in demand. In fact, it has been reported that efforts are being undertaken to improve and manipulate the quality of North American hardwoods.[9] For efficient manufacturing of hardwood products, it is necessary to use different drying methodologies for softwoods and hardwoods. Consideration should also be given to the fact that the dried product quality will vary between these two types of wood; these differences have been reported by Alexiadis et al.[10] Hardwoods have a higher density and this consequently causes greater shrinkage during drying, making this type of wood susceptible to defects such as surface checking, honeycombing, and collapse.[11] Many studies have been reported on checking due to drying in fast-growing trees.

Therefore, the objective of this study was to investigate microcrack morphology in situ in *Melia azedarach*, a fast-growing, ring-porous hardwood that grows in Japan, and also in a diffuse-porous Acacia hybrid that grows in Vietnam. The morphological characteristics of the microcracks occurring in these two woods were then compared.

Materials and methods

Materials and preparation

Natural Acacia hybrid (*Acacia mangium* × *Acacia auriculiformis*) and *Melia azedarach* were used in this study. The Acacia hybrid was a diffuse-porous wood and the boundary of the growth ring was not clearly identifiable. The tree was 8 years old and the breast-height diameter was 12.7 cm; the specific gravity when air-dry was 0.69. Tangential and radial shrinkage were 7.43% and 3.23%, respectively. *Melia azedarach* is a ring-porous wood and the growth-ring boundary was visible; the specific gravity was 0.60. The age of the tree was 13 years and the growth-ring width averaged 6.4 mm.

Two longitudinal, successive specimens were obtained from the green sapwood of each type of wood; 5-mm cubes for Acacia hybrid, and 9-mm cubes, including one with the growth ring, for *Melia azedarach*. One specimen was observed by CLSM and the other was used to measure the moisture content. Two end-matched specimens were used to form a pair of specimens. Transverse surfaces were smoothed using a sliding microtome. Eight pairs of Acacia hybrid specimens and nine pairs of *Melia azedarach* specimens were prepared.

Visualizing method

CLSM was used as described by Sakagami et al.[8] A CLSM instrument and a balance were placed in a controlled-environment chamber where temperature and relative humidity were precisely controlled under preset conditions to visualize the microcracks in situ. In addition, thermolamps were used to maintain an elevated temperature. A steep gradient in moisture content from the surface to the interior of the wood is essential for formation of the microcracks. In order to create such a gradient, adjustments were made to the temperature and relative humidity conditions for each species. The specimens of the Acacia hybrid and *Melia azedarach* were dried at temperatures up to about 60°C and 50°C, respectively. The relative humidity for both species was maintained at levels below 5% using a humidity generator. These respective conditions were suitable for microcrack generation. The relationship between the temperature and relative humidity in the controlled-environment chamber is shown in Fig. 1 and the time history of the decrease in moisture content of all specimens in these conditions is shown in Fig. 2. The green moisture content was between 75% and 95% for Acacia hybrid and between 110% and 145% for *Melia azedarach.* The specimens were dried until the moisture content was less than 5%. It appears that the steep gradient in moisture content was created because the moisture content drastically decreased during the initial 30 min. As a consequence, the formation and

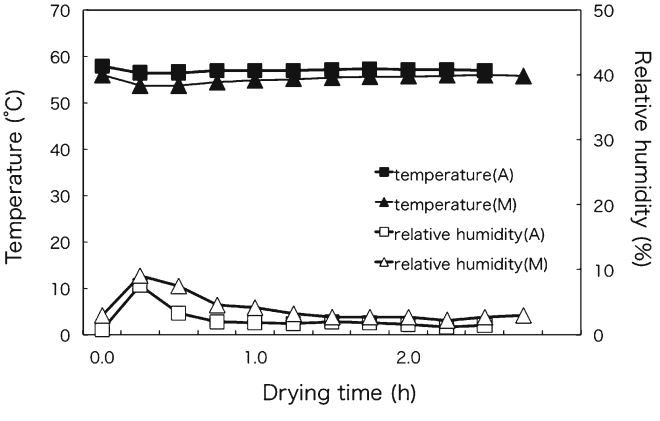

Fig. 1. Temperature and relative humidity in the controlled-environment chamber. *A*, Natural Acacia hybrid (*Acacia mangium* × *Acacia auriculiformis*); *M*, *Melia azedarach*

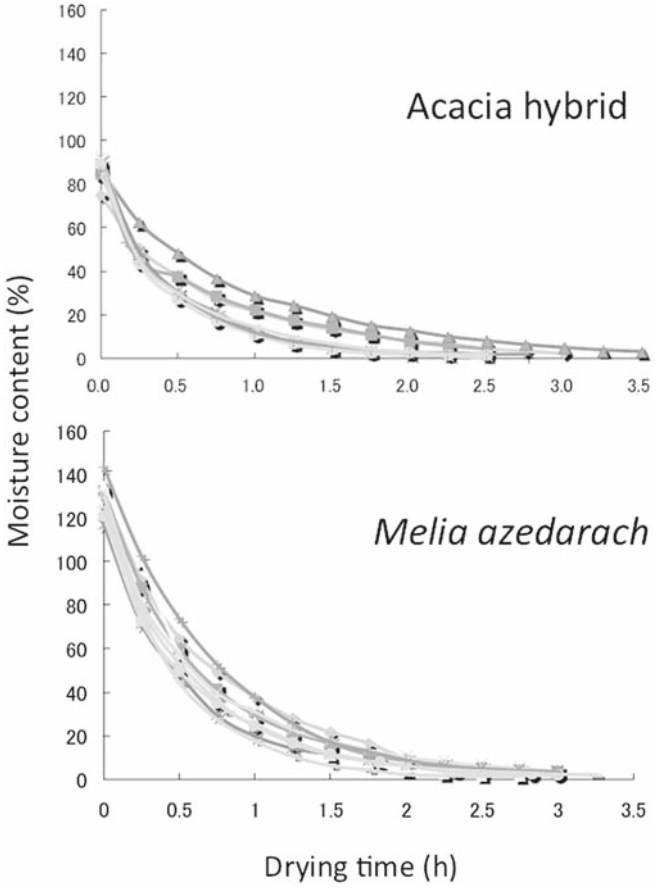

Fig. 2. Relationship between the drying time and moisture content for natural Acacia hybrid (*A. mangium* × *A. auriculiformis*) (*upper*) and *Melia azedarach* (*lower*)

transformation of the microcracks on the surface were observed under these conditions.

After a set of specimens was placed on the stage of the CLSM instrument, they were dried to a constant weight. Three kinds of dry lenses (4×/n.a. 0.2, 10×/n.a. 0.45, and 40×/n.a. 0.95, where n.a. represents the numerical aperture) were selected according to need. Images were obtained at a resolution of 1280 × 1024 pixels and the pixel sizes were 2.36 μm (4×), 0.94 μm (10×), and 0.24 μm (40×). Images were recorded using an Argon ion laser with an excitation wavelength of 488 nm and an emission filter with a 500-nm longpass (HQ500LP). The scan speed was 166 lines per second. Under these conditions, damage on the surface due to the laser could not be detected. Initial images of the surfaces were taken immediately after the specimens were weighed. After microcrack formation was initiated, images were captured every minute until the moisture content reached equilibrium. The moisture content was calculated from the weight of the wood block. The specimens were weighed every 15 min to detect the change in the moisture content. At the last stage of drying, the equilibrium moisture content was less than 5% for all specimens.

Results and discussion

Distribution of microcracks

Using CLSM, the microcracks that formed on the surface of the specimens of both species and propagation of the microcracks were observed in situ as the moisture content decreased. Differences were observed between the Acacia hybrid and *Melia azedarach* with regard to the distribution of the microcracks. In our previous study, we had obtained 1280 × 1024 pixel images of microcracks in specimens of *Cryptomeria japonica* using a 10× lens.[8] Similarly, for the *Melia azedarach* specimens (Fig. 3a), a few microcracks were seen in images obtained at a resolution of 1280 × 1024 pixels using a 4× lens; however, in some cases, only one microcrack could be detected. In contrast, a large number of microcracks were detected on the surface of the Acacia hybrid specimens (Fig. 3b). Most of these microcracks were distributed among every two or three rays. These phenomena were observed in all the specimens.

In situ observation of microcracks

The use of CLSM and the controlled-environment chamber made it possible to observe the transformation of the microcracks when the wood was dried from the green condition to equilibrium moisture content of less than 5%. Differences in the type of microcracks were observed between the Acacia hybrid and *Melia azedarach* specimens.

Acacia hybrid

Sequential images of the Acacia hybrid specimens undergoing a decrease of moisture content are shown in Fig. 4a. The green moisture content of this CLSM specimen was 89.0%. Microcracks were not detected on the surface immediately after the initiation of the drying process (Fig. 4a image 1). After 8 min, microcracks were generated between the wood fiber and ray parenchyma (Fig. 4a image 2), and the moisture content at this point was 68.0% as calculated from the approximated curve in Fig.4a. With further decrease in the moisture content, the microcracks propagated rapidly along the ray parenchyma toward both bark and pith. Thereafter, the propagation of the microcracks slowed, and the progression came to a standstill when the moisture content was 25.1%. The microcracks were the largest at this point (Fig. 4a image 4). The detailed images of the tips of the microcracks are shown in Fig. 5a, b. The tips of the microcracks were seen to have stopped near vessel elements (Fig. 5a) or when they came into contact with neighboring microcracks (Fig. 5b). The same phenomena were observed in all the specimens. With further drying, the microcracks closed. However, they were still observable up to the last stage of drying when the moisture content was reduced to 2.0% (Fig. 4a image 6). For almost all the specimens, the microcracks were identified by CLSM. Similar tendencies were observed for all the specimens.

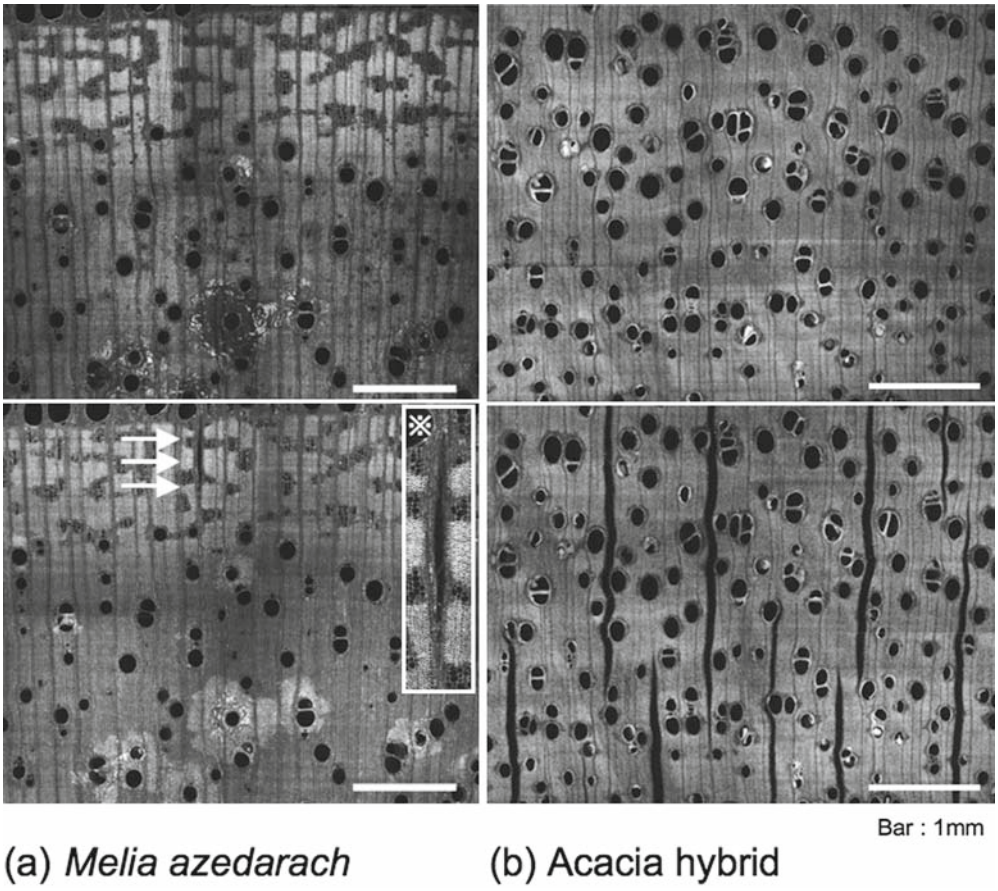

Fig. 3a, b. Distribution of microcracks. The *upper images* were taken during the initial stage of drying and the *lower images* when the microcracks were at their largest. **a** *Melia azedarach*: only one microcrack appeared (*white arrows*) and *inset* shows a detailed view of the microcrack. **b** Natural Acacia hybrid (*A. mangium* × *A. auriculiformis*): numerous microcracks were observed

Melia azedarach

The relationship between the moisture content and microcrack propagation is shown in Fig. 4b. The green moisture content of this CLSM specimen was 141.7%. As was the case with the Acacia hybrid, microcracks could not be detected on the surface immediately after the drying process was initiated (Fig. 4b image 1). After 48 min of drying (the moisture content was 47.3% as calculated from approximated curve in Fig 4b), microcracks were generated between the wood fiber and ray parenchyma in the latewood region (Fig. 4b image 2). Subsequently, the microcracks advanced along the ray parenchyma toward both the bark and the pith; thereafter, the propagation gradually slowed down, and then stopped when the moisture content was 37.4%. This was the point at which the crack reached maximum size (Fig. 4b image 4). The tips of the microcracks that progressed toward the bark halted either at the level of the growth-ring boundary (Fig. 5d) or just before it (Fig. 5c). In contrast, the tips of the microcracks that progressed toward the pith stopped either at a vessel element in the earlywood (Fig. 5f) or just before it (Fig. 5e). In our previous study, microcracks that formed in specimens of *Cryptomeria japonica* that were generated in the latewood region involved the growth-ring boundary and stopped in the earlywood region of the next ring. However, the tips of the microcracks in the *Melia azedarach* specimens were not seen to reach the vessels in the earlywood of the next ring. Subsequently, the microcracks closed and most of them could not be detected by CLSM at the last stage of drying (Fig. 4b image 6).

Morphological characteristics of microcracks

The weak points in the wood structure are classified from many investigations into two categories on the basis of the sites where checks or fracture occur: those between adjacent tracheids and those between the ray parenchyma and tracheid or wood fiber. Tensile testing has been widely adopted to detect weak points in the wood structure. These investigations have revealed that the cracks advance in the radial direction more easily than in the tangential direction, and that they are formed by cell wall peeling[12] and rupture of the interface zone between adjacent tracheids.[13] Analysis at the ultrastructural level revealed that intrawall failure tended to appear either in the compound middle lamella[14,15] or between the S_1 and S_2 layers.[16,17] Oven-dried *Pinus radiata* specimens also exhibit fracture between the compound middle lamella and the S_1 layer.[18] In contrast, it has been reported that the microcracks form between the ray parenchyma and tracheid or wood fiber,[6] as was the case in both this study and our previous study.[8] Perré[6] observed the propagation of cracks in softwood Douglas fir, diffuse-porous beech, and ring-porous oak at the anatomical level. Microcrack formation observed in the latewood region in Douglas fir was also

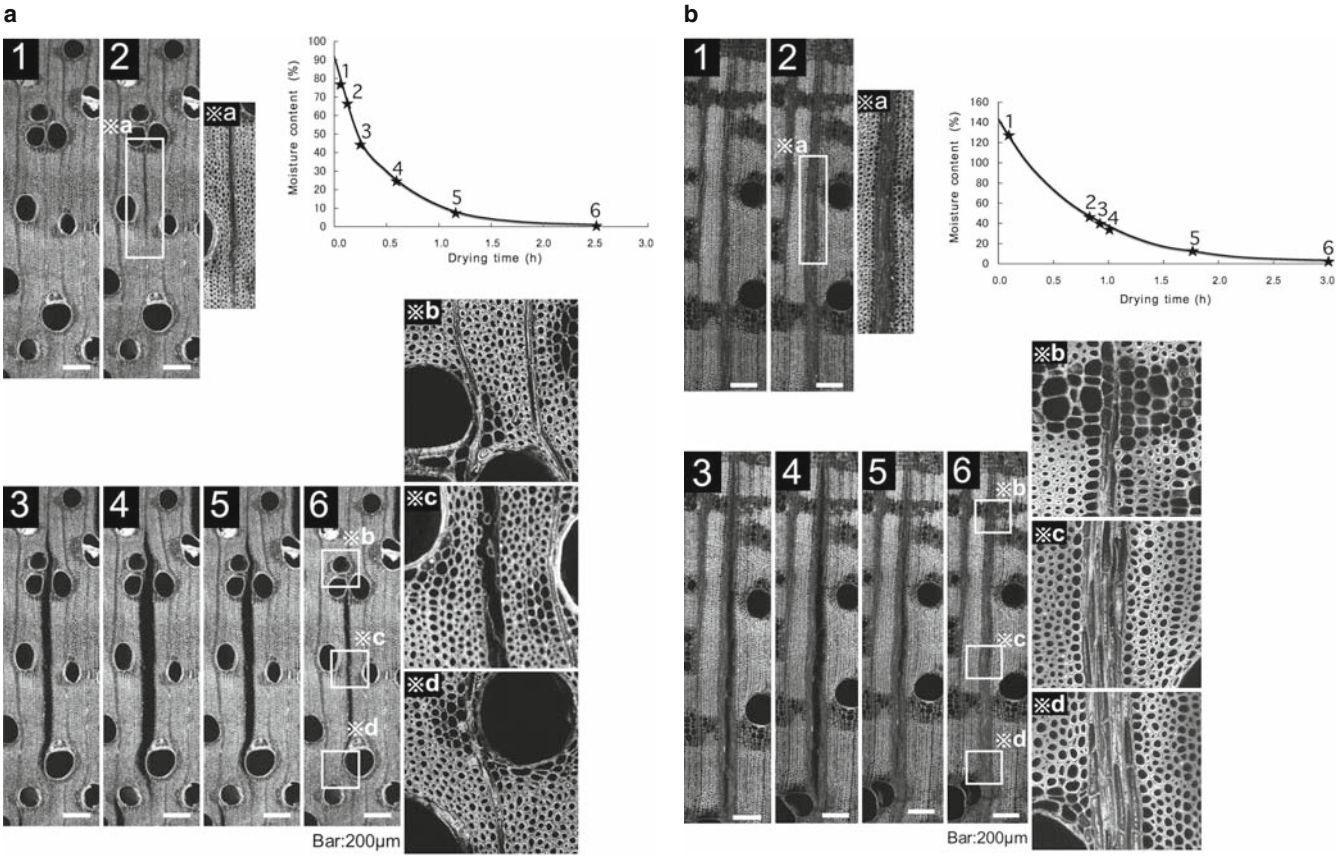

Fig. 4a, b. Relationships between the moisture content and microcracks for **a** natural Acacia hybrid (*A. mangium* × *A. auriculiformis*) and **b** *Melia azedarach. Numbers* on the plots correspond to the numbered images. *Cross section a* is a detailed image of the initial stage of drying. *Cross sections b–d* are detailed images during the final stage of drying

observed. In the case of the diffuse-porous Acacia hybrid, the distribution of microcracks was different from that in beechwood, although in both woods, the microcracks formed in the ray parenchyma were similar. From these studies, we can assume that the growth-ring boundary influences the microcrack morphology. It is known that the shrinkage in the latewood region is greater than that in the earlywood region.[19–21] In cases for which a distinct growth-ring boundary exists on the surface, microcrack formation occurred in the latewood region, where the tangential stress was concentrated. In contrast, there may be no such concentration of tangential stress in the Acacia hybrid in which the growth-ring boundary is not clear. Accordingly, a large number of microcracks were seen on the surface. It has been observed that in some ring-porous woods, microcrack formation occurs in the latewood region and the cracks stopped at the vessels and at the growth-ring boundary (Fig. 5f). In Perré's investigation, checks at the border of the ray parenchyma in ring-porous oak were also reported.[6] Additionally, tangential checks also appeared along the ring-porous zone, although they were not detected in our study.

These differences in the weak points that lie between adjacent tracheids or between the ray parenchyma and tracheid or wood fiber were assumed to result from the differences in the mechanism of crack formation and propagation. In general, tensile failure occurred via intrawall failure. However, the ray parenchyma has also been found to be poor at transmitting tangential tension.[17] Ray parenchyma plays an important role in the formation of microcracks during drying because the surface dries more rapidly and shrinks faster than the interior because the moisture content on the surface decreases very quickly during the initial stage of drying. Therefore, it was inferred that in the case of wood that has a steep gradient of moisture content from the surface to the interior, the weak points on the surface are between the ray parenchyma and tracheid or wood fiber.

Conclusions

Microcracks that developed on the transverse surface during drying were visualized in situ using CLSM for specimens of an Acacia hybrid and *Melia azedarach*. We concluded that the morphological characteristics of the microcracks in Acacia hybrid and *Melia azedarach* can be attributed to the wood structure, in particular, to the presence of a distinct growth-ring boundary. Moreover, one type of weak point on the transverse surface was suggested to be located between the wood fiber and the ray parenchyma.

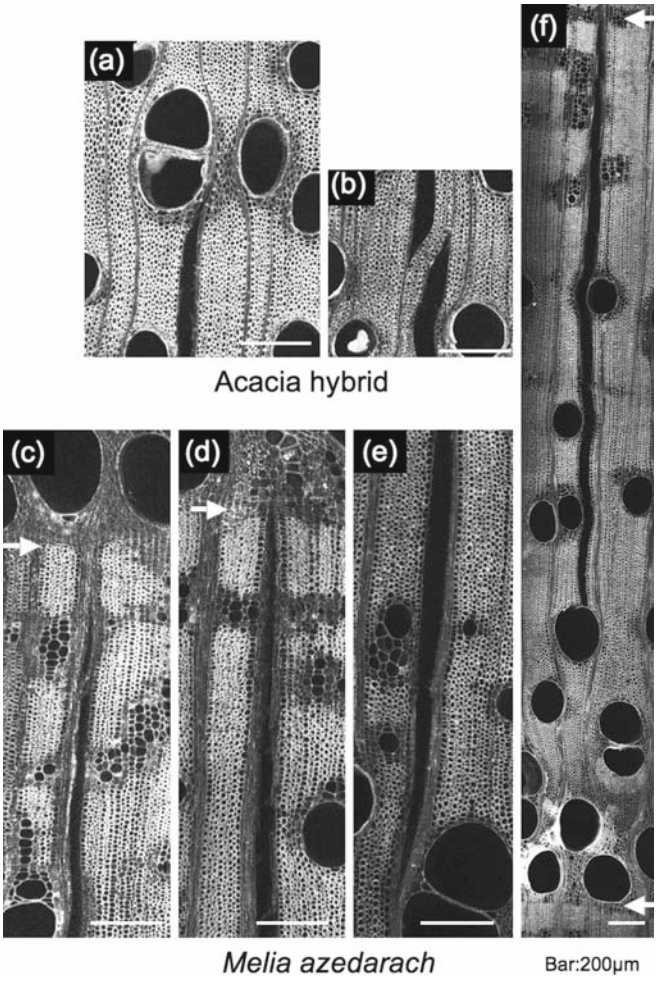

Fig. 5a–f. The point where the microcracks were the largest. **a**, **b** Images of the crack tips in the natural Acacia hybrid (*A. mangium* × *A. auriculiformis*) specimen. **c**, **d** Images of crack tips propagating toward the bark in *Melia azedarach*; **e**, **f** images of crack tips propagating toward the pith in *Melia azedarach*. *White arrows* mark the growth-ring boundary

Acknowledgments This research was supported in part by a Grant-in-Aid for Scientific Research (19580192) from the Ministry of Education, Culture, Sports, Science, and Technology of Japan.

References

1. Keey RB, Langrish TAG, Walker JCF (1999) Kiln-drying of lumber. Springer, Berlin Heidelberg New York
2. Kifetew G, Thuvander F, Berglund L, Lindberg H (1998) The effect of drying on wood fracture surfaces from specimens loaded in wet condition. Wood Sci Technol 32:83–94
3. Thuvander F, Kifetew G, Berglund LA (2002) Modeling of cell wall drying stresses in wood. Wood Sci Technol 36:241–254
4. Wallström L, Lindberg KAH (1999) Measurement of cell wall penetration in wood of water-based chemicals using SEM/EDS and STEM/EDS technique. Wood Sci Technol 33:111–122
5. Wahl P, Hanhijärvi A, Silvennoinen R (2001) Investigation of microcracks in wood with laser speckle intensity. Opt Eng 40: 788–792
6. Perré P (2003) The role of wood anatomy in the drying of wood: "Great oaks from little acorns grow." Proceedings of the 8th International IUFRO Wood Drying Conference, Brasov, Romania, pp 11–24
7. Senft JF, Bendtsen BA (1985) Measuring microfibrillar angles using light microscopy. Wood Fiber Sci 17:564–567
8. Sakagami H, Tsuda K, Matsumura J, Oda K (2009) Microcracks occurring during drying visualized by confocal laser scanning microscopy. IAWA J 30:179–187
9. Cutter BE, Coggeshall MV, Phelps JE, Stokke DD (2004) Impacts of forest management activities on selected hardwood wood quality attributes: a review. Wood Fiber Sci 36:84–97
10. Alexiadis P, Cohen DH, Kozak RA, Avramidis S (2007) Kiln drying Canadian softwoods and hardwoods: different species—different problems. J Inst Wood Sci 17:259–267
11. Milota MR, Smith WB (1994) Contrasting drying practices for hardwoods and softwoods. Drycon: Proceedings of the Wood Technology Drying Management Conference, Vancouver, pp 1–4
12. Thuvander F, Berglund LA (2000) In situ observations of fracture mechanisms for radial cracks in wood. J Mater Sci 35:6277–6283
13. Dill-Langer G, Lütze S, Aicher S (2002) Microfracture in wood monitored by confocal laser scanning microscopy. Wood Sci Technol 36:487–499
14. Debaise GR, Porter AW, Pentoney RE (1966) Morphology and mechanics of wood fracture. Mater Res Stand 6:493–499
15. Korán Z (1967) Electron microscopy of radial tracheid surfaces of black spruce separated by tensile failure at various temperatures. TAPPI 50:60–67
16. Côté WA, Hanna RB (1983) Ultrastructural characteristics of wood fracture surfaces. Wood Fiber Sci 15:135–163
17. Zink AG, Pelikane PJ, Shuler CE (1994) Ultrastructural analysis of softwood fracture surfaces. Wood Sci Technol 28:329–338
18. Putoczki TL, Nair H, Butterfield B, Jackson SL (2007) Intra-ring checking in *Pinus radiata* D. Don: the occurrence of wall fracture, cell collapse, and lignin distribution. Trees-Struct Funct 21:221–229
19. Nakato K (1958) On the cause of the anisotropic shrinkage and swelling of wood. VII. On the anisotropic shrinkage in transverse section of the isolated springwood and summerwood (in Japanese). Mokuzai Gakkaishi 4:94–100
20. Pentoney RE (1953) Mechanisms affecting tangential vs. radial shrinkage. J Forest Prod Res Soc 3:27–32
21. Ma Q, Rudolph V (2006) Dimensional change behavior of Caribbean pine using an environmental scanning electron microscope. Dry Technol 24:1397–1403